Planetary and Space Science 117 (2015) 106–118

Contents lists available at ScienceDirect

Planetary and Space Science

journal homepage: www.elsevier.com/locate/pss

Formation of the "ponds" on asteroid (433) Eros by fluidization

D.W.G. Sears [a,b,*], L.L. Tornabene [c], G.R. Osinski [c,d], S.S. Hughes [e], J.L. Heldmann [a]

[a] NASA Ames Research Center, Planetary Systems Branch (MS245-3), Mountain View, CA 94035, USA
[b] Bay Area Environmental Research Institute, NASA Ames Research Center, Mountain View, CA 94035, USA
[c] Department of Earth Sciences and Centre for Planetary Science and Exploration, University of Western Ontario, London, ON, Canada N6A 5B7
[d] Department of Physics and Astronomy, University of Western Ontario, London, ON, Canada N6A 5B7
[e] Department of Geosciences, Idaho State University, Pocatello, ID 83209, USA

ARTICLE INFO

Article history:
Received 4 October 2014
Received in revised form
18 May 2015
Accepted 20 May 2015
Available online 29 May 2015

Keywords:
Eros
Ponds
Vesta
Phreatic craters
Fluidization
Craters

ABSTRACT

The "ponds" on asteroid (433) Eros are fine-grained deposits approximating flat (quasi-equipotential) surfaces with respect to local topographic depressions (e.g., craters) in spacecraft images. These ponds are discussed in the context of laboratory simulation experiments, crater-related ponded and pitted deposits observed on Mars and Vesta, terrestrial phreatic craters, and degassing features associated with eroded impact craters on Earth. While the details of formation of these features on Mars, Vesta and the Earth are thought to be different, they all include mechanisms that require the interactions between surface materials and volatiles (e.g., water vapor). Indeed, analogous features similar to the Eros ponds can be reproduced in the laboratory by the release of vapor (ice sublimation, water evaporation, or N_2) through an unconsolidated regolith (independent of regolith composition). Eros is widely thought to be dry, but the discovery of exogenic water on Vesta, and recent arguments that subsurface water might be present in the inner asteroid belt suggest that endogenic water might also be present and serve as a source of the gases produced in the ponds. The amount of water required is comparable to the amount of water observed in little-metamorphosed ordinary chondrites (a few wt%). The primary morphologic characteristics of the Eros ponds can be explained in this model. The heat source for degassing could have been solar heating following transfer from a main belt orbit to a near Earth orbit. Although other hypotheses (e.g., electrostatic levitation, seismic shaking, and comminution of boulders) can account for most of the features of the ponds, recent observations regarding the role of volatiles on planetary surfaces, our laboratory experiments, and fluidization deposits on active comets suggests that degassing is a reasonable hypothesis to be considered and further tested for explaining the Eros ponds, and similar features on other bodies.

1. Introduction

The "ponds" on asteroid (433) Eros appear to be flat-topped fine-grained deposits that embay and fill local topographic depressions – most often craters. They were observed early in the NEAR-Shoemaker mission during its one-year orbital exploration of Eros and they were found to be ubiquitous (Robinson et al., 2001, 2002). An example is shown in Fig. 1. Most noteworthy is the flatness of the ponds, which Robinson et al., and others, have suggested to be perpendicular to the gravity field, although the gravity field is complex and not that well known. Similarly, the ponds are often displaced from the center of the depression in which they are located and are gravitationally controlled, i.e. a crater inclined to the local gravitational potential will have an off-set pond. However, recent work suggests this may not be as straightforward as previously suggested (Roberts et al., 2014a). The morphology of the ponds is fairly uniform, but spectroscopically the surface of the ponds is slightly blue relative to the surrounding plains, suggesting a finer grain size or younger regolith (less space "weathered") material (e.g., Heldmann et al., 2010). Sometimes they appear streaked, suggesting perhaps grain sorting during movement or mass movement after emplacement. Robinson et al. (2001) also observed that the ponds have a radius that is typically one-third of the radius of the host depression, and they are fairly shallow, only 5% of the depth of the host depression, so the amount of material is small relative to the crater volume. They observed that the ponds are concentrated along the subsolar points and in regions of low gravity (Fig. 2) may be an artifact of image resolution as these regions are where the spacecraft was especially close to the surface (Roberts et al., 2014b). Otherwise, this potential relationship between pit concentration and the sub-

* Corresponding author at: Bay Area Environmental Research Institute, NASA Ames Research Center, Space Science and Astrobiology Division (MS245-3), Mountain View, CA 94035, USA. Tel.: +1 510 258 8595/2323.

http://dx.doi.org/10.1016/j.pss.2015.05.011
0032-0633/

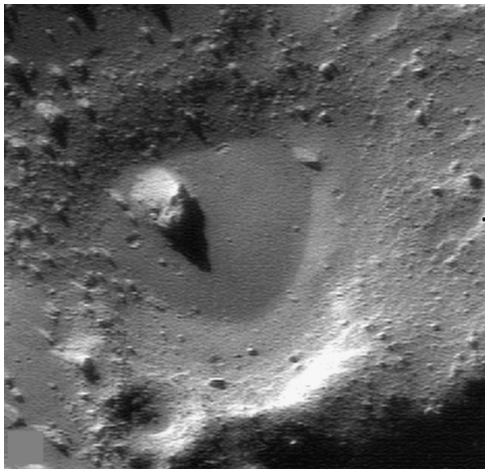

Fig. 1. Example of a typical pond at the bottom of a crater on Eros containing a prominent boulder. The field of view is 220 m and the location of the crater is 179.04°W, 2.42°S. (NASA/JHU, image MET 155888598, resolution 0.55 m/pixel).

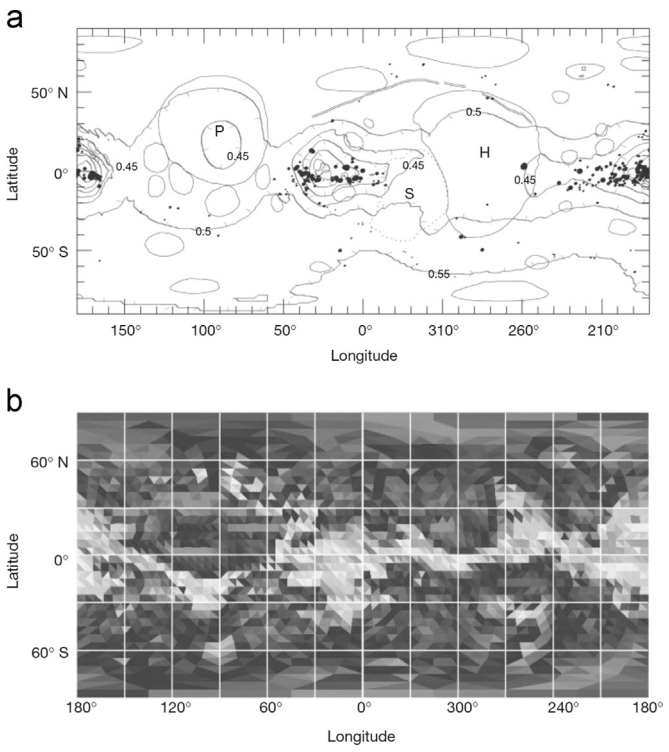

Fig. 2. (a) Map of Eros showing the location of ponds (dots), the craters Psyche (P), Shoemaker (S), and Himeros (H), and gravity contours (labeled 0.55, 0.5, and 0.45 cm s^{-2}; unlabeled closed contours at 170°W and 20°W are 0.25 and 0.30 cm s^{-2}, respectively). Ponded deposits are found preferentially in regions of relatively low gravity. (b) The amount of time an area receives direct sunlight (85–90° incidence angle) on a relative scale; darkest least, lightest most. The distribution of ponds follows the locus of the Sun across the Eros sky. (From Robinson et al., 2001, where the original color versions of these figures may be found). Roberts et al. (2014b) suggest that this correlation is an artifact caused by higher image resolutions when the spacecraft is closest to the asteroid.

solar point not only suggests mass transport, but also a dependency on solar insolation. Placing further constraints on the emplacement and formation of ponds on asteroids may reveal important clues with respect to surface process and the evolution of small solar system bodies.

When the ponds were first described, Robinson et al. (2001) suggested that they were formed by the electrostatic levitation and transport of dust, a possibility anticipated for asteroids by Lee (1996) and similar to the process that has been described for the Moon (Gold and Williams, 1973; Stubbs et al., 2005; Poppe and Horanyi, 2010). This would account for most of the ponds' physical properties, especially their possible dependence on insolation. However, despite obtaining clear images of the horizon, the NEAR-Shoemaker spacecraft a "horizon glow" similar to that observed on the lunar surface and was thought to be an evidence of the electrostatic levitation mechanism on the Moon (Stubbs et al., 2005, for a brief summary and some recent ideas in the lunar case). This does not preclude possible electrostatic activity in the past.

Cheng et al. (2001a) rejected the idea that electrostatic processes were the cause of the ponds and instead suggested that "seismic shaking", movement due to the vibrations caused by meteorite impacts, caused the mass movement of fine surface materials to locations of low gravity. The movement and concentration of fine-grained material in the aftermath of an impact had been previously described by Cintala et al. (1979). This idea has gained much support and has been invoked to explain regions of fine-grained material on several other asteroids (e.g. Itokawa, Miyamoto et al., 2007; Lutetia, Vincent et al., 2012). We note that electrostatic levitation and boulder comminution (see below) would also require some form of seismic shaking (Roberts et al., 2014a).

However, Dombard et al. (2010) argue that since ponds are observed in regions of low slope and high elevation, seismic shaking is unlikely. Instead, they observed that there were normal boulders associated with the ponds, this is the case in the example in Fig. 1, and suggested that it was the impact-induced comminution of boulders inside craters that caused the ponds rather than mass transport material into the crater. Boulders are a commonplace on Eros and are ubiquitous across its surface (Durda et al., 2012). The association of boulders with ponds may be coincidental, as we mentioned above, or observational biases since boulders tend to readily stand out on the flat surface of a pond.

In several cases, it has been suggested that the Yarkovsky effect caused movement of dust from the poles to the equator of small asteroids (e.g. Marchi et al., 2010). As yet, Yarkovsky redistribution of dust has not been associated with the formation of ponds, although this is also possible.

Most of the properties of the Eros ponds reflect the mobilization of surface regolith in a way that concentrates the fine-grained fractions near the surface and within the depressions. The behavior of granular flows was reviewed at some length by Jaeger and Nagel (1992) and depends on the particles and the containers. Robinson et al. (2001) noted that ponded deposits on Eros drape and pile up against pre-existing topography and showed pictures of a topographically isolated crater with a small interior pond, showing that the ponded material did not flow in surrounding terrain. Cheng et al. (2001b) also stated that isolated ponds could be found without a nearby debris flow on Eros and thus ponds could be adjacent to debris flow by chance rather than by co-generation.

Most of the mechanisms for explaining the Eros ponds proposed to date, besides fluidization, involve dry-mobilization of materials. Whereas, Kareev et al. (2002) and Haseltine et al. (2006) suggested that the trigger to flow could be the release of volatiles from the interior of the asteroid. Franzen et al., (2003) and Moore et al. (2003) performed experiments under microgravity conditions and found these fluidization effects were impossible to avoid. Once triggered, they needed very little in the way of a carrier gas. They also described how "waves" of granular material can embay the sides of obstacles (e.g., crater walls in the case of Eros). The role of volatiles during energetic events like impact (e.g. Kirsimäe and Osinski (2013); Stöffler et al., 2013; Artemieva et al., 2013) and volcanism (e.g. Hughes et al., 1999) has recently been discussed by many workers and is also demonstrated by the presence of "pits"

within bodies of impact melt-bearing deposits on Mars (Tornabene et al., 2012; Boyce et al., 2012) and even Vesta – a body previously thought to be extremely dry (Denevi et al., 2012). The Vesta ponded and pitted deposits occur both on the crater floor and, to a lesser extent, on ejecta blankets which are similar in fashion to the ones observed on Mars and impact melt deposits around well-preserved lunar craters. Results from the gamma ray and neutron detector (GRaND) on the Dawn orbiter (Prettyman et al., 2012) shows that the craters that possess these deposits occur where hydrogen concentrations are the highest on the body, suggesting a link with volatiles (Denevi et al., 2012). There has therefore been increasing appreciation of the role of volatiles on planetary surfaces, including small solar system bodies. In conference abstracts, Kareev et al. (2002) and Hasseltine et al. (2006) describe the formation of laboratory analogs of the Eros ponds by degassing of fine powers in a planetary environmental chamber. Here, we discuss these laboratory simulation experiments in the light of recent discussions of volatile behavior during energetic events on planetary surfaces.

2. Volatile-produced structures in the laboratory on Mars and Vesta, during terrestrial impact and during terrestrial volcanism

2.1. Laboratory simulations

2.1.1. Theoretical background

The interaction of volatiles and solid particles is reasonably well understood because of its importance in industrial processes (e.g. Kunii and Levensiepel, 1991) and pyroclastic volcanism (e.g. Parfitt and Wilson, 2008). An interesting example of how laboratory measurements can help understand pyroclastic emplacement is the study of Wilson (1980). Quantitative treatments for size and density sorting have been invoked to explain the chondrule size distributions in meteorites (e.g. Whipple, 1972a, 1972b; Dodd, 1976; Rubin and Keil, 1984), the metal distribution in chondrites (Schneider et al., 2003), and the formation of the chondrite classes which are driven largely by the size and density sorting of chondrules and metal grains (e.g. Huang et al., 1996; Akridge and Sears, 1999). The process is best described by the Ergun equation, which equates the upward drag on the particulates by the flowing gas to the downward force on the particulates due to gravity:

$$\frac{1.75R_e^2}{\varepsilon^3\phi} + \frac{150(1-\varepsilon)R_e}{\varepsilon^3\phi^2} = \frac{d^3\rho_g(\rho_s-\rho_g)g}{\mu^2} \quad (1)$$

where R_e is the Reynolds number, ε is the void fraction under minimum flow conditions, d is the particle size, ρ_g and ρ_s are the gas and solid particle densities, ϕ is the sphericity, g is the acceleration due to gravity, and μ is the viscosity. Typical values for these parameters and results are given by Huang et al. (1996) and Akridge and Sears (1999). Essentially, the flow rates needed to obtain fluidization on a 10-km asteroid with particulate properties similar to chondrites are very low, say 0.1–1.0 mm/s.

2.1.2. Experimental setup

An unexpected observation made during measurements of the evaporation rate of water under a variety of simulated Mars-like conditions (Chevrier et al., 2007) provided the basis for the present idea that Eros ponds might be the result of gas-driven fluidization. The equipment consisted of a cooled cylinder 2 m high and 21 cm in diameter, which was evacuated to about 0.1 mbar (where 1 mbar = 100 Pa) and, normally, filled with a CO_2 atmosphere to 6 mbar (Sears and Chittenden, 2005; Sears and Moore, 2005). However, for the present observations the pressure was determined by gas release rates and remotely observing the surface; it sometimes reached 300 mbar. Water or ice was buried under layers of four different types of regolith simulant (Table 1): (1) the Mars regolith simulant, JSC Mars-1, (2) the tephra used to produce JSC Mars-1 but in its natural state (with 11 vol% adsorbed water), (3) crushed basalt, and (4) crushed phyllosilicates. The powders had a broad range of grain sizes between ~20 μm and ~300 μm. The JSC Mars-1 simulant is a Hawaiian tephra from Pu'u Nene, a volcanic cone at 1850 m elevation on Mauna Kea's south flank that has been dried and sieved. It was obtained from Carl Allen, Johnson Space Center, Houston. The preparation of the simulant and its physical and chemical properties were described in detail by Allen et al. (1998). We also obtained a 50 gal drum of the same material to use in our large scale chamber experiments. The basalt is the same as that used in our experiments to explore the behavior of water under a basaltic regolith (Bryson et al., 2008) and the phyllosilicates were the same as those used in the work of Chevrier et al. (2008). In addition, experiments to simulate processes on asteroidal regoliths used a simulant consisting of quartz and iron filings with chondritic Fe/Si ratio. Details of these chondrite simulant experiments were reported by Franzen et al. (2003) and Moore et al. (2003). In experiments most relevant to the present paper, quartz pebbles (0.5–1 cm in size) were placed on the surface to simulate a coarse-grained fraction (i.e. "boulders"). In all cases, the depth of the simulated regolith was typically 40 cm.

Table 1
Experiments in the planetary environmental chamber.

Expt.	Soil simulant	Volatile source	Atmosphere pressure (mbar)
A	Mars-1	20 g ice, in open glass containers	300
B	Mars-1	20 g water, in permeable containers	0.3–300
C	Mars-1	20 g ice	0.3–300
D	Mars-1	1 g of ice	0.3–300
E	Tephra	none	0.3–300
F	Sand	N_2 gas, via tube	0.3–300
G	Sand	N_2 gas, via tube	0.3
H	Basalt	Undetermined amounts of ice and water	6
I	Phyllosilicates	Undetermined amounts of ice and water	6

The behavior of the simulant as pressure was reduced in the chamber was monitored by video cameras installed 15 cm and 30 cm above the surface. An Ocean Optics visible spectrometer, with a range of 400–950 nm, was mounted outside the chamber but observed the surface through a light guide to ~10 cm vertically above the volatile source in the regolith. After the experiment, the chamber was opened and photographs were taken of the surface being careful not to disturb the regolith. However, because of the geometry of the set-up, photographs could only be taken normally to the surface using normal lighting.

2.1.3. Results

As the chamber was evacuated, there was a sudden onset of "fluidization" of the regolith when pressures reached ~10–300 mbar at 0 °C and pumping rates of 0.37–0.57 L/s. There was a clear and reproducible sequence. First, there was a sudden onset of churning of the regolith. Second, there was the generation of a "plume" of fine-grained dust. Churning would typically continue for some time, but with decreasing intensity with time. Typically it would take 30 min for a 250 mL water supply to be exhausted. To simulate this behavior when using N_2, we would slowly turn off the supply after about 30 min. Third, a depression would slowly

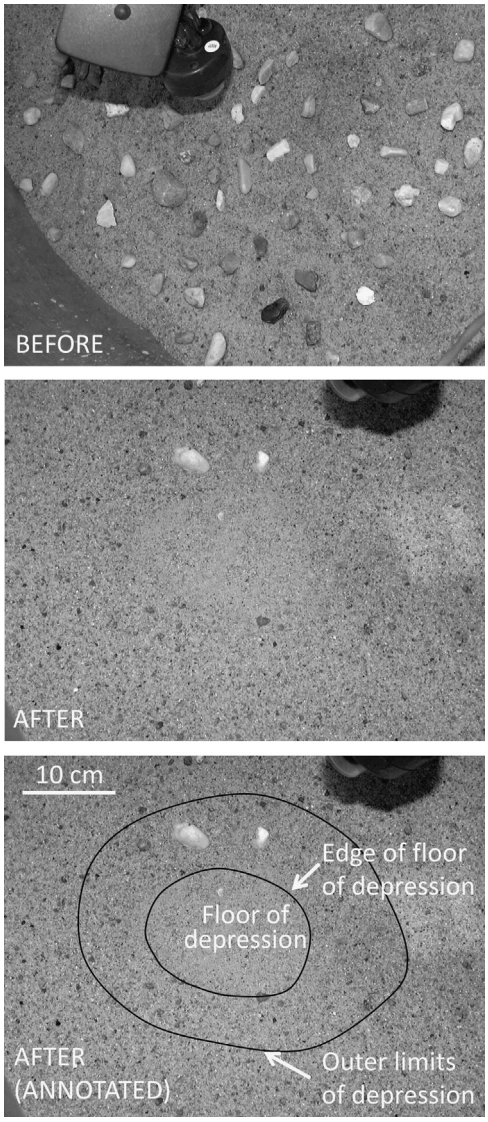

Fig. 3. One g fluidization experiments on the surface of loose unconsolidated sand. Top, the original surface with centimeter-sized pebbles sitting on a coarsely sieved surface of Hawaiian tephra. Middle, the surface after water vapor has been allowed to pass through the mixture. Pebbles have disappeared, a bowl shaped depression has formed, and the bottom of the depression has been filled with a deposit of fine grains. Bottom, since these images were taken under vertical illumination-making it difficult to see the structures – we show a sketch to guide the eye. The outer contour indicates the limits of the depression; the inner contour indicates the region of fine-grained deposits. The field of view is about 35 cm.

form over the volatile source as the plume became weaker. It was clear from the real-time video as soon as a depression formed, it had a flat floor that was covered with a bright layer of fine-grained material. The larger grains and the pebbles, originally present on the surface, disappeared although outside the rim of the depression they were still at or near the surface (Fig. 3). The final structure was very similar to the NEAR-Shoemaker images of pond deposits within small craters on Eros (c.f., Figs. 1 and 3). We show a cartoon of this process in Fig. 4.

Upon opening the chamber and dissecting the regolith, the missing pebbles were found to have sunk towards the source of volatiles or migrated outside the depression. In fact, there appeared to be a cone of mobilized material, centered on the volatile source, with the depression at the surface in the center of the cone and pebbles generally buried but at the edge of the mobilized cone of material. The flat surface within the depression consisted of a ~3–4 mm layer of fine grains, which coarsened and thickened towards the crater walls. While initially the surface of the regolith simulant had a fairly uniform increase in abundance with grain size up to 300 μm, after the experiment there was a sharp peak in grain size at ~50 μm (Fig. 5).

The sorting behavior observed during degassing was essentially independent of the composition of the regolith simulant. Likewise, replacing water vapor with nitrogen gas produced the same results. The behavior of the bed and the particle sorting is clearly a purely a physical process that does not depend on the composition of the solid or vapor. We concede that in the present experiments our substrates were fairly similar and fairly homogeneous in density. Particle-size sorting occurs rapidly in fluidized beds that are mixtures of differing size and density (Huang et al., 1996; Franzen et al., 2003; Moore et al., 2003).

In the case of the natural tephra, where there was no localized source of volatiles but the water adsorbed uniformly throughout the regolith layer, low levels of churning occurred throughout the regolith sample. Again there were "plumes" that decreased in intensity with time and ceased observable activity at about the same time as the rest of the regolith.

Under the atmospheric pressures and temperatures of our experiments, the equilibrium state of water is ice although our experiments involve continuous pumping and so conditions are not at equilibrium. During most of our experiments, water vapor was probably being produced by both vaporization of liquid water and the sublimation of ice. Even for experiments in which we started with liquid water, the water quickly froze due to adiabatic cooling. The ice continues to sublimate, but at a slower rate than at the onset of vaporization. For about 72 h after the beginning of the experiment, we could recover blocks of ice near the location of the original water or ice source. After about a week or more we found only dry soil.

In addition to increasing the abundance of fine grains on the surface, the degassing process increased the reflectivity of the surface without changing the spectrum (Fig. 6). A similar brightening due to decrease in grain size of the regolith was observed by Heldmann et al. (2010).

2.2. *Possible Martian analog observations.*

Densely pitted crater-related deposits associated with 204 craters, occasionally including ponded deposits behind terraces and on the ejecta blankets, were recently observed on Mars; the pits are attributed to the release of volatiles due to the interaction between subsurface water/ice and impact-generated surface materials, i.e., highly shocked rock and impact melt deposited following an impact (Tornabene et al., 2012). The pits are polygonal to quasi-circular features (Fig. 7), ~10 m to 3 km in size, in craters 1–150 km in diameter, distributed around the planet at latitudes between 53°S to 62°N. Boyce et al. (2012) likened the texture and pattern of multiple overlapping pits to a froth and explained their formation in terms of explosive degassing of water from water-bearing, impact melt-rich breccia at the time of deposition, consistent with the interpretation of Tornabene et al. (2012). These authors also likened these features with the segregation channels, or vent pipes, observed in cross-section with outcrops of eroded suevite deposits at the Ries impact crater in Germany.

There are, of course, numerous differences with respect to the formation of environment of the pits on Mars and the ponds on Eros. On Mars, the target surface contains a considerable amount of volatiles; Mars is a much bigger object, and there is a measureable atmosphere – although the atmosphere appears to be unimportant for pit formation based on current formation models (Boyce et al., 2012), and consistent with their observation on Vesta (Denevi et al., 2012). Their relevance to our proposed mechanism

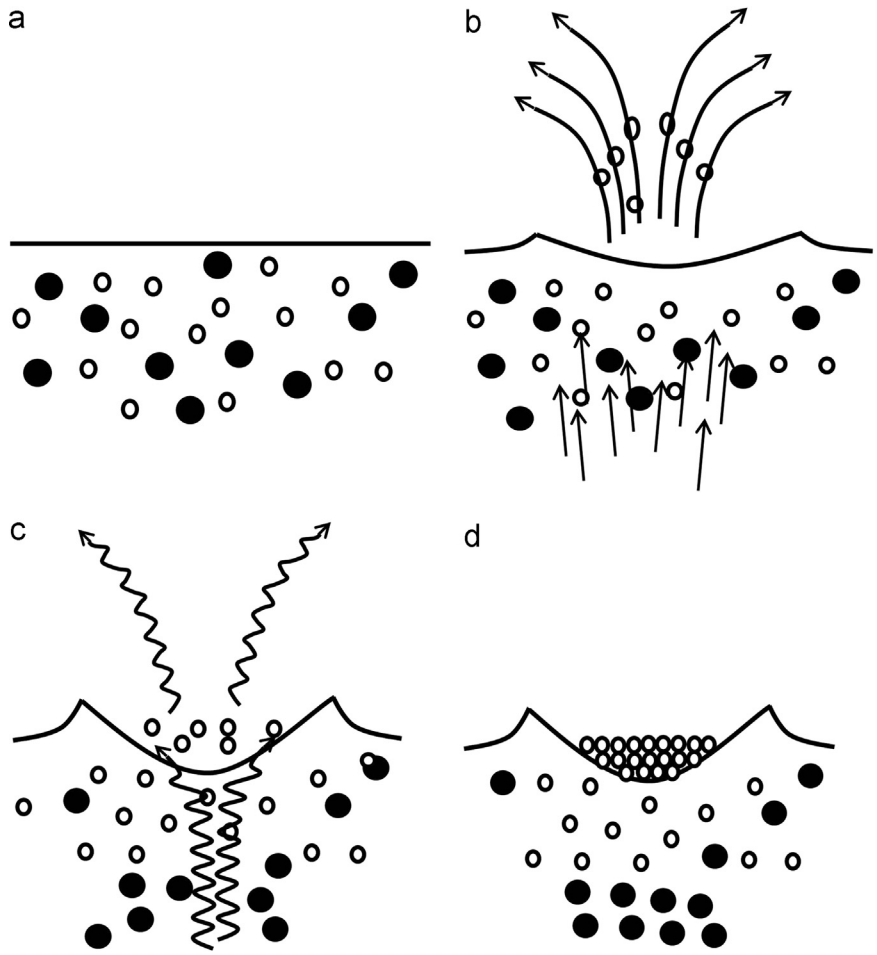

Fig. 4. Cartoon describing the method by which a ponded crater is formed during fluidization of an unconsolidated regolith containing a mixture of grain sizes. (a) Initial bed of coarse and fine grains. (b) The release of volatiles from depth causes finer grains to be lifted out of the bed sculpting a shallow crater-like depression as mass is lifted and lost (elutriated) or falls back at the peripheries of the vent. (c) As gas flow attenuates, a crater is formed due to the collapse of the once fluidized bed and smaller grains are no longer carried aloft. (d) The final situation is a crater-like depression filled with a flat layer of fine grains. A variation on this theme is that the crater hosting the pond was formed by an impact that excavated volatile-rich material and brought it closer to the surface where it degassed and fluidized the surface grains.

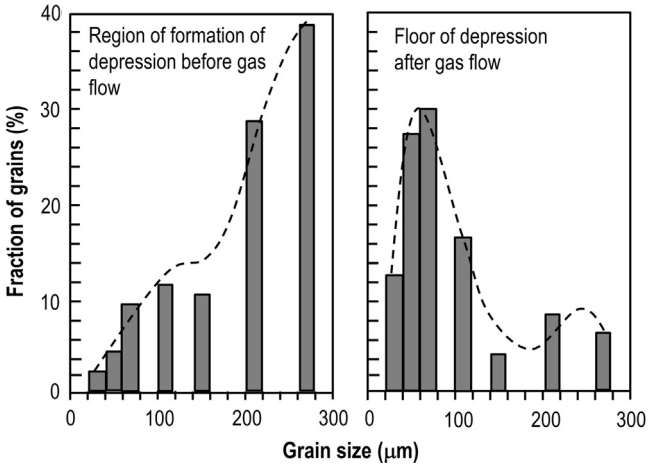

Fig. 5. Observed size distribution of grains in the mock regolith simulant before and after degassing. Originally the surface of the regolith simulant was dominated by grains in the 200–220 and 266–280 μm sieve fractions, but after flow of water vapor through the bed, within the new circular depression formed by the degassing the coarse grains disappeared and the bed became dominated by grains in the 40–80 μm sieve fractions. The fine grains filled the depression caused by the slow termination of the gas flow. Lines are best fits of polynomial equation (b-spline).

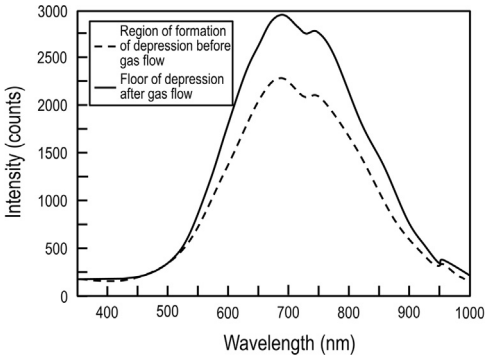

Fig. 6. Visible spectra for the surface of the regolith simulant before and after the degassing experiment in the circular depression formed by the gas flow. The surface showed a significant increase in reflectivity after the experiment without any significant change in the spectrum.

for the formation of the Eros ponds is that both are a manifestation of processes occurring during the loss of volatiles from a low- to non-cohesive and "fluidized" surface.

2.3. Possible Vesta analog observations

Arguably the biggest surprise of the visit by the Dawn spacecraft to the dwarf planet Vesta was that it found evidence for

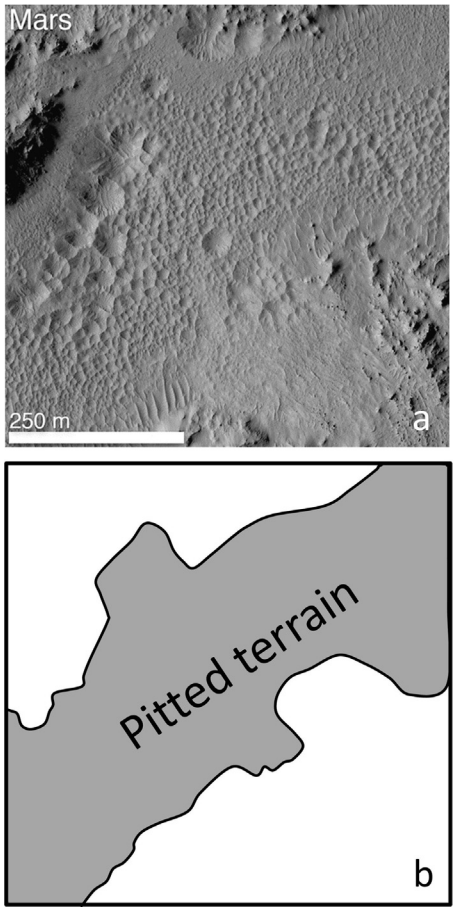

Fig. 7. (a) Image of crater-related pitted materials on the floor of the ~28 km diameter martian crater Tooting obtained by the HiRISE instrument on Mars Reconnaissance Orbiter. (NASA/JPL/UA PIA 16185). (b) A key identifying the pitted terrain.

volatiles on the surface of this basaltic, and what was otherwise considered to be a dry lunar-like planetary object. This was a surprise despite the long-known presence of abundant volatile-rich CM chondrite-like clasts in the howardites (Wilkening, 1973), basaltic breccias from Vesta (Drake, 2001). CM chondrites contain up to ~10 vol% water, although the clasts in howardites are dehydrated, presumably during or subsequent to emplacement. There is at least one vesiculated eucrite, but McCoy et al. (2006) suggested that the volatile was CO or CO2 since the meteorites were currently dry. However, the presence of CM clasts suggests that was not always the case. In any event, De Sanctis et al. (2012) reported 2.8 μm OH bands in the visible/near IR spectrum of Vesta, suggestive of hydrated minerals, which are located in low albedo regions. The GRaND instrument on Dawn also detected hydrogen in the low albedo regions (Prettyman et al., 2012). The low albedo regions are explained by McCord et al. (2012) as deposits of exogenic carbonaceous materials – probably low angle and low velocity impactors of CM chondrite-like materials. Clearly, there is ample evidence that volatiles were present during some of the igneous or melt phase history of Vesta.

Scully et al. (2012) claimed to have found gully-like features on the inside walls of craters on Vesta which may be attributed to fluid/volatile-abetted processes; although, in a more recent publications by these and other authors they interpreted the low sinuosity flows as dry mass wasting (Scully et al., 2013) or dry flows (Krohn et al., in press). Less controversial is the observation of crater-related pitted terrain on Vesta (Fig. 8), reported by Denevi et al. (2012), which are nearly identical both morphologically and morphometrically to those observed on Mars (Tornabene et al., 2012). As with Mars, the pitted terrain consists of irregular pits, which are thought to form by degassing of volatile-bearing material heated by impact. Again, Vesta is a bigger object with an older surface than Eros, but the surprise existence of presumably exogenic water on Vesta does prompt the question of whether surprise exogenic water might be present in smaller amounts on other asteroids.

2.4. Possible impact analog observations

While surface conditions on Earth and Mars are very different, there has been an increased interest recently in the role of volatiles during meteorite impacts on Earth. The effect of target lithology on the products was recently reviewed by Osinski et al. (2008) who point out that while similar amounts of melt are produced by impact into crystalline and sedimentary targets, the melt products appear very different. The presence of volatile components in the target increases melt viscosity and increases the possibility of explosive reactions. Newsom et al. (1986) also described numerous fluidization effects observed in the field at the Ries Crater in southern Germany (Fig. 9). Most noteworthy are pipe structures (or channels) that were produced when the escape of volatiles formed conduits to the surface through suevite deposits (i.e., impact-melt-bearing breccias). Unpublished fieldwork by one of the present authors (GO) shows: (1) that these features are not distributed evenly throughout the ejecta, and (2) the 'pipe structures' are typically decimeters across and several meters long. We do not know the original scale of the Ries degassing features, nor their surface manifestations, because surface degradation processes and vegetation have obscured the story. About half of the known terrestrial impact craters show signs of hydrothermal activity resulting from interactions between volatiles and target materials (Kirsimäe and Osinski, 2013). Vapor dominated reactions occur early in the process (to produce garnet, epidote, and feldspar), and liquid dominated reactions occur last (to produce carbonates, sulfides, and Fe-oxyhydrates), with vapor-liquid reactions producing phyllosilicates at intermediate conditions. The presence of both pipe structures and hydrothermal minerals indicates that volatiles are released by processes associated with the impact event.

The proposed mechanism for forming the Eros ponds is possibly more analogous to the fluidization pipes at the Ries Crater than the other analogs. The Ries fluidization channels are produced when fluids released from depth found their way to the surface. The surface expression of the channels has been removed by erosion and obscured by vegetation, but one might expect a broadening out and an infill of fine-grained material. Under the lower gravity of an asteroid, one might expect more elutriation of fine grains.

2.5. Possible volcanic analog observations

While clearly no volcanism has occurred on Eros, it is possible that the phreatic craters, or the maars, may have some level of analogy to the present proposal that the Eros ponds are the result of fluidization processes. The effect of volatiles on volcanic processes has long been known because of the devastating effect of historic *nuées ardents* (e.g. Parfitt and Wilson, 2008). Well-documented examples of phreatic craters are found, for example, at the Craters of the Moon National Monument and Preserve (Fig. 10; Hughes et al., 1999; Greeley et al.,1977a; Greeley and Schultz, 1977; Womer, 1977). Probably the best known of these lies on the Great Rift and is known as Kings Bowl, which was formed 2,220 ± 100 years ago when a magmatic dike encountered subsurface water. The resulting explosion created an 85 m long, 30 m wide and 30 m

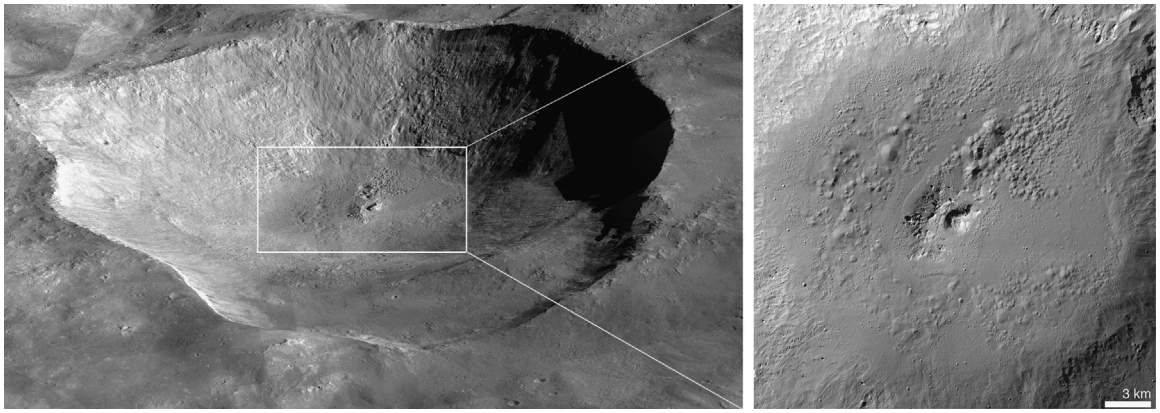

Fig. 8. The 70 km crater Marcia on Vesta whose floor contains pitted terrain produced when volatiles were released from a melt during the later stages of impact. Image obtained by the Framing Cameras on the Dawn spacecraft. Note the difference in geometry of the two images; the detail is foreshortened relative to the image on the right. (NASA/JPL PIA 16182).

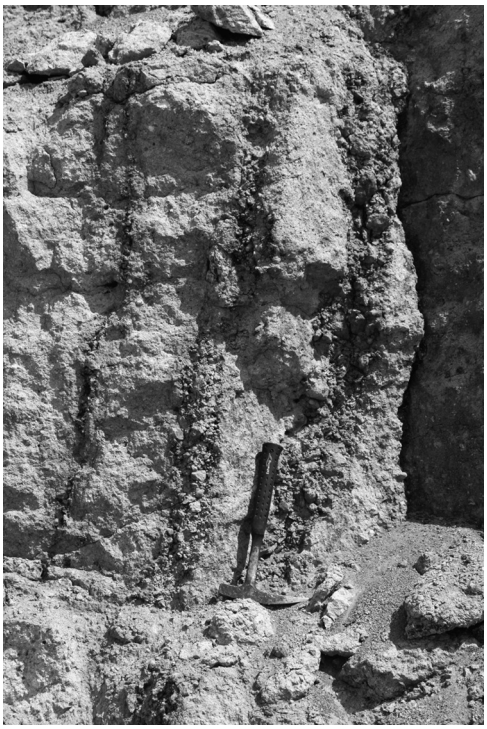

Fig. 9. Three channels, or degassing pipes, from an outcrop at the Ries crater, in southern Germany, formed by the elutriation of fine particles as volatiles were released from a once fluidized bed. Rock hammer for scale. (Photograph by Gordon Ozinski).

deep crater and ejected blocks to distances in excess of 100 m. It is probable that boulders were originally scattered in all directions, but deposits from a large tephra cloud have obscured the blocks towards the east. Other phreatic pits have been described on the lava fields in the vicinity of Craters of the Moon. Some have been smoothed over by loess and surrounded by subsequent flows (China Cap), some show evidence for multiple events (Split Butte). Kings Bowl is more deep rooted and exposes underlying strata.

The phreatic volcanic craters differ from the pits on Mars and Vesta because in the terrestrial case the lavas encountered water, whereas on Mars and Vesta the water was dissolved in the melts. Thus the reaction that produced the Kings Bowl was more explosive than the processes producing the Vesta and Mars pits which were more like a bubbling oatmeal or froth. The main point however, is that the phreatic craters are another indication of the widespread nature of features on planetary surfaces produced when volatiles interact with surface materials. However, other forms of phreatic features are maars, one of the best examples of which is the famous Ukinrek Maars, in Alaska (Kienle et al., 1980). Maars are shallow, broad, low-rimmed explosion craters formed by phreatic and phreatomagmatic eruptions with crater diameter to rim height ratios are usually about 10:1 or less. The infill is fine-grained, typically 0.2–2 mm.

3. Discussion

With a growing interest in the effects of volatile behavior on the surfaces of planetary bodies, we reexamine the suggestion of Kareev et al. (2002) and Hasseltine et al. (2006) that the formation of the Eros ponds might be related to the release of volatiles through an unconsolidated regolith. These volatiles could be endogenic, released from depth through channels caused fractures in the crust, or excavated by impact, or they could be exogenic, brought onto the asteroid by the impact of water-rich (CM-like) projectiles.

3.1. Comparative planetary degassing and pit-like structures

Of course, while there are similarities between the present experiments, the Vesta and Mars pits, the phreatic craters and the degassing at impact sites, there are notable differences. The ponded and pitted deposits on Mars and Vesta most probably represent the release of endogenic volatiles trapped within the melt-bearing breccias and released during the interaction of impact with the target (on Vesta or Mars). In the case of the Kings Bowl phreatic crater, it was the melt coming suddenly into contact with water that produced an explosion and resulted in a crater. The impact process differs from the volcanic process in which water and ice can be incorporated quite suddenly into impact-melt bearing deposits (i.e,, during the impact processes); this is because the excavation flow is perpendicular to the shock front, which effectively allows molten silicate to be excavated and deposited along with very low shock materials such as ice and water-rich materials. The sudden generation of such a deposit would immediately react to reach thermal equilibrium and the volatiles would be rapidly released to react physically and chemically with the rocks and melts, either as vapors or condensed liquid.

Thus, while processes during impact, volcanism, or insolation induced degassing are very different, the latter stages of these processes on Mars, Vesta, and the Ries are somewhat analogous in that they all involve the behavior of volatiles in conjunction with cohesive materials and involve some aspects of fluidization. After

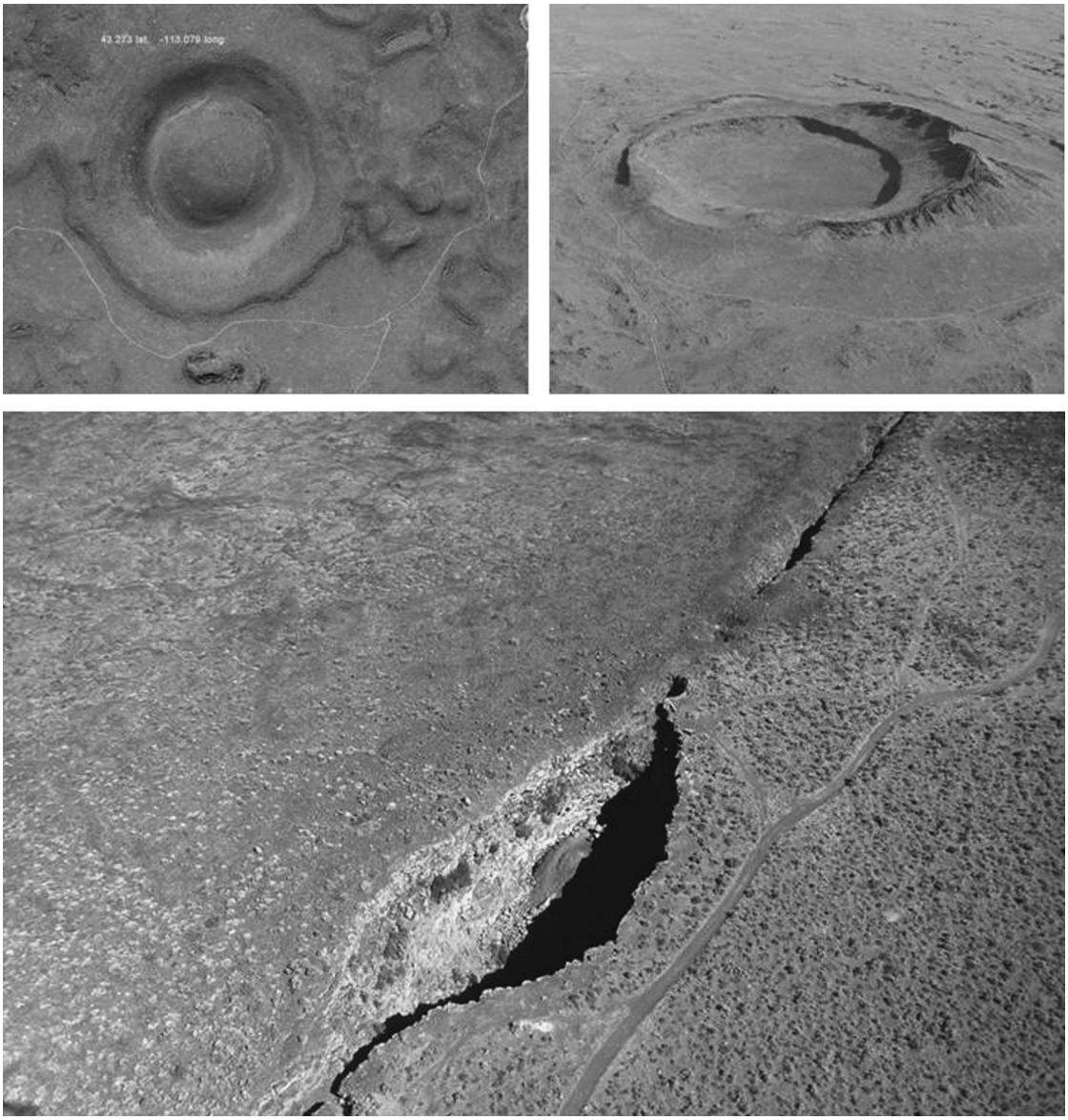

Fig. 10. Phreatic craters at the Crater of the Moon National Monument and Preserve. Top left, China Cap (265 m rim-to-rim, 240 m inside diameter), top right, Split Butte (600 m in diameter), bottom, Kings Bowl (90 m by 30 m). China Cap is covered with later lava, and Split Butte represents two events. Kings Bowl is the most recent event and ejecta blocks can be seen, especially on the west. These structures appear to be analogous to the pits on Vesta and Mars and might be expected to be present on the surface of many NEAs where water-bearing material is present. (China Cap image from Google Earth, Split Butte image was taken by Susan Sakimoto and Scott Hughes, Kings Bowl is a national Parks Service image.).

formation and emplacement, by whatever process, the volatile-rich deposits continue to slowly release volatiles to produce the structures observed.

3.2. Comparison of laboratory with the Eros ponds

According to Robinson et al. (2002), the major properties of the Eros ponds are that (1) they have distinctive flat floors sometimes showing non-central downside movement, (2) they have sharp boundaries, (3) they have uniform morphology, color and albedo, (4) they typically have a radius ~1/3, the diameter of the host crater and a depth ~5% of the host crater diameter and that they are not concentrations of a uniform widespread ejecta, and (5) they can be seen on other (non-crater) depressions. Additionally, the Eros depressions appear preferentially at the locus of the sub-solar point and they are more abundant in regions of lower gravity, however we note again that the conclusion that the ponds are preferentially located at loci of the subsolar point has been challenged (Roberts et al., 2014b).

The model structures in our laboratory experiments have most of the morphologic attributes described earlier. The morphogies formed in our chamber are flat, uniform, structures with sharp boundaries and they have depth to diameter ratios of ~5%. It is important to distinguish that we did not attempt to create these features in craters, but crater-like depressions formed and the fine-grained deposits tended to build up within them during our degassing experiments. This is in agreement with experiments by Mills (1972), which showed that a slow attenuation of the gas flow through a fluidized bed could create crater-like features. This does not mean that these features are never associated with craters, which could excavate volatiles and cause fluidization in crater bottoms. We probably have both, fluidization-produced "craters" with ponds and fluidization-produced ponds at the bottom of impact craters. Our simulated ponds showed all of the physical features of the Eros ponds except (1) the presence of boulders in

the ponds, and (2) the spectral differences between the ponds and the surrounding plains – both of which already have explanations.

The absence of boulders (i.e. the centimeter-sized quartz pebbles in our case) is explained in two ways. First, it can be ascribed to the thickness of regolith in our experiments. Our experiments provided a greater depth to which boulders could sink within the fluidized bed; whereas the fine deposits in the ponds on Eros are constrained within the crater bowl. The concentration of boulders on the surface during fluidization is a mechanical effect that occurs in locations where movement is restricted so that fines can move freely but boulders cannot. This is sometimes referred to as "the Brazil nut effect" (Asphaug et al., 2001). Second, the presence of boulders on Eros can be explained as a result of the ubiquitous distribution of boulders over the surface of Eros caused by a major impact on a low gravity body (Thomas et al., 2001). In fact, the distribution of ejecta from the impact that produced the Shoemaker Crater (Thomas et al., 2001) resembles the distribution of ponds, especially in its equatorial concentration.

Our experimentally produced "ponds" differ from the Eros ponds in that the ponds on Eros appeared slight bluer than the surrounding regions. We infer from this that the blue nature of the ponds on Eros reflects their youth relative to the surrounding materials, rather than grain size (REF); in contrast, space weathering is known to redden chondrite-like surfaces on asteroids (e.g. Clark et al., 2002). Performing these fluidization experiments with chondritic regolith might clarify the cause of the color difference.

3.3. Water on Eros?

There are two ways in which water could reside on or near the surface of Eros. (1) There could be endogenous subsurface deposits rich in water, either as ice or chemically bound water, as seems to be the case for Ceres (Küppers et al., 2014). (2) There could be exogenous sources of water brought to the asteroid by volatile-rich impacts, just as appears to be the case for Vesta (e.g., Prettyman et al., 2012; De Sanctis et al., 2012a).

The clues to asteroid interior composition and structure, and whether it is water-bearing, are bulk density and meteorite compositions:

Bulk densities: The bulk densities of asteroids range from 1.2 to 4.4 g/cm^3 (1 g/cm^3 = 1000 kg/M^3) with S asteroids averaging 2.4 g/cm^3 and C asteroids averaging 1.8 g/cm^3 (Table 2; Viateau and Rapaport, 2001). This is considerably below grain densities and usually assumed to indicate that the asteroids are highly porous. However, these low densities could also be a result of significant amounts of free or bound water; whether free or bound, the effect on bulk density is the same. Fig. 11 shows the calculated density for asteroids, with anhydrous grain densities of 3.5 g/cm^3 and containing various amounts of water and with diverse porosity. The bulk density of C asteroids can be explained by a composition similar to C chondrites, with ~10–20 vol% water, and porosity of ~25–35 vol% (Table 3). A more significant comparison is S asteroids with ordinary chondrites whose predicted porosity assuming anhydrous asteroids is ~25%, a factor of three or four larger than observed for ordinary chondrites. Ordinary chondrite porosities range from ~1% to ~18%, with averages of 6.4%, 4.5%, and 7.9% for H, L, and LL chondrites, respectively (Britt and Consolmagno, 2003). Ordinary chondrite porosities would require ~20 vol% water (~2.2 wt%), to be present in the asteroid to match bulk density. In short, the bulk densities alone do not preclude significant water in Eros-like asteroids; it is simply the prevailing view that water was absent in objects that formed inside the "snowline". As we showed above, the amounts of water vapor required to produce ponds on the surface of an asteroid by fluidization are quite low.

Table 2
Asteroid densities (Britt et al., 2002).

Asteroid	Class	Density (g/cm^3)
1 Ceres	G	2.12 ± 0.04
2 Pallas	B	2.71 ± 0.11
4 Vesta	V	3.44 ± 0.12
10 Hygeia	C	2.76 ± 1.2
11 Parthenope	S	2.72 ± 0.12
15 Eunomia	S	0.96 ± 0.3
16 Psyche	M	2.0 ± 0.6
20 Massalia	S	3.26 ± 0.6
22 Kalliope	M	2.5 ± 0.3
45 Eugenia	F	$1.\ 2^{+0.6}_{-0.2}$
87 Sylvia	P	1.62 ± 0.3
90 Antiope	C	1.3
121 Hermione	C	1.96 ± 0.34
243 Ida	S	2.6 ± 0.5
253 Matthilde	C	1.3 ± 0.2
433 Eros	S	2.67 ± 0.03
704 Interamnia	F	4.4 ± 2.1
762 Pulcova	PC	1.8 ± 0.8
804 Hispania	PC	4.9 ± 3.9
1999 KW4		2.39 ± 0.9
2000 DP107	C	$1.\ 62^{+1.2}_{-0.9}$
2000 UG11		$1.\ 47^{+0.6}_{-1.3}$

Mean C ~1.8, mean S ~2.4, V 3.4.

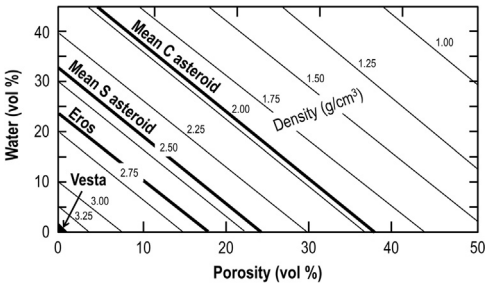

Fig. 11. Mass balance calculations for a porous body composed of silicates and ice, constrained by bulk density. The amount of water (as ice or chemically bound water) is plotted against porosity for asteroids indicating the resultant density, assuming a grain density of 3.5 g/cm^3. Also shown are the average densities for S and C asteroids and the densities for Eros and Vesta (asteroid densities from Britt et al. (2002)). This diagram says nothing about the stability of ice, but simply po ints out that if water is present (as ice or hydrated silicates) it is possible for the discrepancy between bulk density and grain density to be explained by the presence of water as well as porosity.

Meteorite compositions: The meteorites most similar to Eros, on the basis of present spectral interpretations, are the ordinary chondrites (Bell et al., 2002). These are generally noted for their dryness, but the vast majority of ordinary chondrites in our collections are also noted for the high levels of metamorphism they have suffered. However, the least metamorphosed ordinary chondrites contain water, perhaps 3%, (Wiik, 1969; Jarosewich, 1990). In fact, water content is used as a parameter for assessing the levels of parent body metamorphism experienced by a given meteorite (Dodd et al., 1967; Van Schmus and Wood, 1967; Sears et al., 1980). The least metamorphosed ordinary chondrites contain traces of hydrated minerals and minerals formed in an aqueous environment that can be observed petrographically (Hutchison et al., 1987; Grossman et al., 2000). The most successful thermal models for the interiors of asteroids involve internal heat sources (such as ^{26}Al) with the least metamorphosed, water-bearing, meteorites closest to the surface of the asteroid (e.g. Akridge and Sears, 1998).

Villas (1994) and Merényi et al. (1997) have shown that the 3 μm absorption band is present in many asteroids suggesting the presence of water, which they assumed to be water of hydration

Table 3
CI and CM chondrites and their water contents and densities.

Meteorite	Class	Water		Porosity		Bulk density	
		wt%	Ref.	Vol%	Ref.	g/m^3	Ref.
Alais	CI	19.62	1	2	3		
Ivuna	CI	43.47	1				
Orgueil	CI	16.9	2	11.3	3	2.11 ± 0.12	3
ALH 81302	CM	12.94	2				
ALH 83100	CM	13.38	2				
Benten	CM	10.7	2				
Cold Bokkeveld	CM	15.3	1	12.9	3	2.31	3
Erakot	CM	19.26	1				
Essebi	CM	9.9	1				
Haripura	CM	36	1				
Mighei	CM	2.16	1	28.2	3	1.94 ± 0.03	3
Murchison	CM	10.09	2	17.1	3	2.37 ± 0.02	3
Murray	CM	12.51	1				
Nawapali	CM	16.56	1				
Santa Cruz	CM	10.44	1	30.3	3	1.79	3
Staroje Boriskino	CM	0.99	1				
Yamato 791824	CM	12.5	2				
Yamato 793321	CM	9.23	2				

1 Wiik (1969)
2 Jarosewich (1990)
3 Britt and Consolmagno (2003).

Table 4
Asteroids with spectroscopic evidence for water on their surface (Villas, 1994).

Asteroid class	Number in sample	Percentage indicating water of hydration	Mean albedo of hydrated asteroids
A	5	0	–
B	18	33.0	0.049
C	128	47.7	0.051
D	35	0	0.041
E	12	0	–
F	36	16.7	0.042
G	7	85.7	0.077
I	3	0	–
M	31	6.5	0.155
P	36	8.3	0.036
Q	1	0	–
R	1	0	–
S	201	0.5	0.095
T	6	0	–
V	1	0	–
X	54	5.6	–

(Table 4). Ceres, a dwarf planet in the outer asteroid belt, appears to be releasing water vapor, especially near perihelion (A'Hearn and Feldman, 1992; Küppers et al., 2014). Rivkin and Emery (2010) and Campins et al. (2010) have found spectroscopic evidence for water on asteroid 24 Themis and proposed that water may be present in the interiors of asteroids closer to the Sun than previously thought. These data are consistent with theoretical estimates that suggest water could survive in the main belt for the age of the solar system if sufficiently buried under a regolith layer (Fanale and Salvail, 1989; Schorghofer, 2008).

The age of the surface of Eros, determined from the crater density, is ~2 Ga (Chapman et al., 2002). On the other hand, the typical lifetime for an asteroid in near-Earth orbit is ~50–100 Ma (Michel et al., 1998), which means that the NEA population must be continually fed from the main belt or cometary sources. The mean temperature of the surface of an S asteroid at ~3 AU is 135 K (making the usual assumptions, e.g. McKeever and Sears, (1980)), below the temperature needed to retain water (Schorghofer, 2008). The mean temperature at 1 AU is ~234 K, at which temperature water will evaporate at a rate depending on depth and physical properties of the regolith. During the transfer from 3 AU to 1 AU the vapor pressure of water increases about seven orders of magnitude (from $\sim 10^{-8}$ mbar to ~0.22 mbar). It is thus possible that the loss of water occurred after moving closer to the Sun and it will have occurred preferentially at the sub-solar points where the Eros ponds are concentrated. Alternatively, water can subsequently be exposed by small impacts over the history of the body

Because the surface of Eros is so much younger than Vesta, and Vesta is a much larger object compared to Eros (~X%), CM-like deposits of material, and concomitant water concentrations, should not be expected to be present in the same amounts on Eros and Vesta. Nevertheless, CM-like material does appear to be common in the asteroid belt (Gaffey et al., 1993) and xenolithic meteorite breccias do show a strong preference towards CM-like projectiles (Wilkening, 1973). So a small component of CM-like material on Eros might be expected, hidden from the NEAR-Shoemaker instruments by a regolith coating or the similarity in composition of CM-like material and Eros surface material; both are essentially chondritic. The black boulder on Itokawa (Saito et al., 2006) might be part of a CM-like projectile

Finally, it might be useful to recall that at least one model for the formation of the dozen or so classes of chondrites involves density and size sorting of the chondrite components (chondrules, metal, and matrix) by a fluidization process on the surface of asteroids (Huang et al., 1996; Akridge and Sears, 1998; Sears, 2005). This hypothesis assumes that asteroids were originally mostly CI or CM-like, with solar compositions, chondrule-poor (or free), abundant water with concomitant mineralogy (phyllosilicates, amorphous phases, evaporates), but dehydration of the surface by impact and sorting by fluidization produced S asteroid-like surfaces and the chondrite classes.

Our experiments suggest that ponded deposits can occur on virtually all small bodies in the solar system that possess volatiles and cohesive materials. Regolith is common and thick on all asteroids imaged to date, but the abundance of volatiles in asteroids is, at present, largely unknown, although there is increasing theoretical and observational evidence that water might be more stable than previously thought. In addition, we note that the regolith is subject to complex interactions, such that structure generated by one process, such as fluidization, can and will be modified by subsequent processes, including space weathering and comminution, and possibly electrostatic levitation and seismic shaking.

3.4. Testing the hypothesis

The properties of the Eros ponds and the simulation experiments are consistent with the ponds being formed by fluidization. Furthermore, we now consider volatiles important in volcanic or impact processes on the surfaces of asteroids. An important question is how do we test the present hypothesis? Do we expect water to be present in the sediments of the ponds, under our favored formation model? Even on Earth, where gravity is higher and water availability is higher, it is difficult to detect water in the fine-grained sediments of maars. Samples from the famous Ukinrek Maars, in Alaska, are generally water-free, reaching 0.14 wt% in only one case out of six (Kienle et al., 1980). Thus it seems doubtful that water will ever be detected in the fine sediments of the Eros ponds remotely or with returned samples. What will be needed are cores that pass through the ponds, reaching bedrock, where rocks from the source region for the purported volatiles may still contain traces of water.

3.5. A comment about comets

Comets are volatile-rich objects that undergo orbit changes similar to that discussed here in connection with onset of outgassing from Eros. It seems reasonable to ask whether there is evidence for fluidization in the images obtained by spacecraft of the nuclei of comets. Comet P/Wild 2 was encountered by the Stardust spacecraft in January 2004 and obtained images showing large circular "craters" with flat bottoms. Brownlee et al. (2004) offered several explanations for these, one of which was that they were the result of fluidization of fine grained materials. The Comet 9 P/Tempel 1 had flow deposits (Thomas et al., 2013) that might arguably be the result of fluidization processes (Belton and Melosh, 2009). Laboratory simulation experiments also suggest that it is gas-dust interactions that cause mobilization of the dust at cometary nuclei (Sears et al., 1999). Fluidization phenomena have also been recently reported on the comet 67 P/Churyumov–Gerasimenko (Thomas et al., 2015).

4. Conclusions

We conclude that while all of the earlier proposed mechanisms for the formation of the ponds on Eros seem to be able to explain all or most of their major properties, recent work on the role of volatiles and fluidization, recent observations on planetary and cometary surfaces, and the similarity of the features produced in the laboratory to the Eros ponds, strongly suggests that fluidization associated with degassing should also be considered as possible explanations. The vapors to drive this process could be either endogenic water trapped at the time of accretion or exogenic water from low angle and low velocity impact of volatile-rich meteorites. Unmetamorphosed ordinary chondrites contain a few weight percent water, sufficient to drive fluidization on small bodies. Surface features caused by the interaction of surface materials with gasses produced by various volatile-releasing mechanisms are common to many planetary surfaces, even though there are many differences in the details of the interactions and the details of the final products.

Acknowledgments

We are grateful to M. S. Kareev, P. H. Benoit, J. D. Haseltine, M. A. Franzen, J. Hanley, and J. Thompson, then at the Keck Lab, for help with the experimental portions of this work and for discussions, and Steve Saunders for his help in securing equipment and for many years of advice, friendship, and encouragement. We are also grateful to James H. Roberts, Johns Hopkins University, Applied Physics Laboratory, for a very helpful review. Certain portions of this work were performed in the Keck Laboratory for Space Simulation, Arkansas Center for Space and Planetary Science, University of Arkansas, which is supported by the University of Arkansas, the W.M. Keck Foundation, the National Science Foundation, and the National Aeronautics and Space Administration. Support to prepare the present paper was provided by a grant from the NASA (Grant no. 13-SSERVI13-0018) Solar System Exploration Research Virtual Institute to the FINESSE team (Field Investigations to Enable Solar System Science and Exploration), Jennifer Heldmann, PI.

References

A'Hearn, M.F., Feldman, P.D., 1992. Water vaporization on Ceres. Icarus 98, 54–60.

Allen, C.C., Jager, K.M., Morris, R.V., Lindstrom, D.J., Lindstrom, M.M., Lockwood, J.P., 1998. Martian soil simulant available for scientific, educational study. EOS 79, 405–412.

Akridge, D.G., Sears, D.W.G., 1998. Regolith and megaregolith formation of H-chondrites: thermal constraints on the parent body. Icarus 132, 185–195.

Akridge, D.G., Sears, D.W.G., 1999. The gravitational and aerodynamic sorting of meteoritic chondrules and metal: experimental results with implications for chondritic meteorites. J. Geophys. Res. 104, 11,853–11,864.

Asphaug, E., King, P.J., Swift, M.R., Merrifield, M.R., 2001. Brazil nuts on Eros: size-sorting of the asteroid regolith. In: Proceedings of the Lunar and Planetary Science XXXII 2001, Abstract #1708.

Artemieva, N.A., Wünnemann, K., Krien, F., Reimold, W.U., Stöffler, D., 2013. Ries crater and suevite revisited—observations and modeling Part II: modeling. Meteorit. Planet. Sci. 48, 590–627.

Bell, J.F.I.I.I., Clark, B.E., Izenberg, N., Lucey, P.G., Clark, B.E., Peterson, C., Joseph, J., Carcich, B., Harch, A., Bell, M.E., Warren, J., Martin, P.D., McFadden, L.A., Wellnitz, D., Murchie, S., Winter, M., Veverka, J., Thomas, P., Robinson, M.S., Malin, M., Cheng, A., 2002. Near-IR reflectance spectroscopy of 433 Eros from NIS instrument on the NEAR mission. Icarus 155, 119–144.

Belton, M.J.S., Melosh, J., 2009. Fluidization and multiphase transport of particulate cometary material as an explanation of the smooth terrains and repetitive outbursts on 9P/Tempel 1. Icarus 200, 280–291.

Boyce, J.M., Wilson, L., Mouginis-Mark, P.J., Hamilton, C.W., Tornabene, L.L., 2012. Origin of small pits in martian impact craters. Icarus 221, 262–275.

Britt, D.T., Consolmagno, G.J., 2003. Stony meteorite porosities and densities: a review of the data through 2001. Meteorit. Planet. Sci. 38, 1161–1180.

Britt, D.T., Yeomans, D., Housen, K., Consolmagno, G., 2002. Asteroid density, porosity, and structure. In: Bottke Jr., W.F., Cellino, A., Paolicchi, P., Binzel, R.P. (Eds.), Asteroids III. University of Arizona Press, Tucson, pp. 485–500.

Brownlee, D.E., Horz, F., Newburn, R.L., Zolensky, M., Duxbury, T.C., Sandford, S., Sekanina, Z., Tsou, P., Hanner, M.S., Clark, B.C., Green, S.F., Kissel, J., 2004. Surface of young jupiter family comet 81P/Wild 2: view from the stardust spacecraft. Science 304, 1764–1769.

Bryson, K.L., Chevrier, V., Sears, D.W.G., Ulrich, R., 2008. Stability of ice on Mars and the water vapor diurnal cycle: experimental study of the sublimation of ice through a fine-grained basaltic regolith. Icarus 196, 446–458.

Campins, H., Hargrove, K., Pinilla-Alonso, N., Howell, E.S., Kelley, M.S., Licandro, J., Mothé-Diniz, T., Fernández, Y., Ziffer, J., 2010. Water ice and organics on the surface of the asteroid 24 Themis. Nature 464, 1320–1321. http://dx.doi.org/10.1038/nature09029.

Chapman, C.R., Merline, W., Joseph, J., Thomas, P.C., Cheng, A.F., Izenberg, N., 2002. Impact history of Eros: craters and boulders. Icarus 155, 104–118.

Cheng, A.F., Izenberg, N., Chapman, C.R., Zuber, M.T., 2001a. Ponded deposits on asteroid 433 Eros. Meteorit. Planet. Sci. 37, 1095–1105.

Cheng, A.F., Barnouin-Jha, O., Zuber, M.T., Veverka, J., Smith, D.E., Neumann, G.A., Robinson, M., Thomas, P., Garvin, J.B., Murchie, S., Chapman, C., Prockter, L., 2001b. Laser altimetry of small-scale features on 433 Eros from NEAR-Shoemaker. Science 292, 488–491.

Chevrier, V., Sears, D.W.G., Chittenden, J.D., Roe, L.A., Ulrich, R., Bryson, K., Billingsley, L., Hanley, J., 2007. Sublimation rate of ice under simulated Mars conditions and the effect of layers of mock regolith JSC Mars-1. Geophys. Res. Lett. 34, L02203. http://dx.doi.org/10.1029/2007GL028401.

Chevrier, V., Ostrowski, D.R., Sears, D.W.G., 2008. Experimental study of the sublimation of ice through an unconsolidated clay layer: implications for the stability of ice on Mars and the possible diurnal variations in atmospheric water. Icarus 196, 459–476.

Cintala, M.J., Head, J.W., Wilson, L., 1979. The nature and effects of impact cratering on small bodies. In: Gehrels, T., Matthews, M.S. (Eds.), Asteroids. University of Arizona Press, Tuscon, pp. 579–600.

Clark, B.E., Hapke, B., Pieters, C., Britt, D., 2002b. Asteroid space weathering and regolith evolution. In: Bottke Jr., W.F., Cellino, A., Paolicchi, P., Binzel, R.P. (Eds.), Asteroids III. University of Arizona Press, Tucson, USA, pp. 585–599.

De Sanctis, M.C., Ammannito, E., Capria, M.T., Tosi, F., Capaccioni, F., Zambon, F., Carraro, F., Fonte, S., Frigeri, A., Jaumann, R., Magni, G., Marchi, S., McCord, T.B., McFadden, L.A., McSween, H.Y., Mittlefehldt, D.W., Nathues, A., Palomba, E., Pieters, C.M., Raymond, C.A., Russell, C.T., Toplis, M.J., Turrini, D., 2012a. Spectroscopic characterization of mineralogy and its diversity across vesta. Science 336, 697–700. http://dx.doi.org/10.1126/science.1219270.

Denevi, B.W., Blewett, D.T., Buczkowski, D.L., Capaccioni, F., Capria, M.T., De Sanctis, M.C., Garry, W.B., Gaskell, R.W., Le Corre, L., Li, J.Y., Marchi, S., McCoy, T.J., Nathues, A., O'Brien, D.P., Petro, N.E., Pieters, C.M., Preusker, F., Raymond, C.A., Reddy, V., Russell, C.T., Schenk, P., Scully, J.E.C., Sunshine, J.M., Tosi, F., Williams, D.A., Wyrick, D., 2012. Pitted terrain on Vesta and implications for the presence of volatiles. Science 338, 246–249.

Dodd, R.T., 1976. Accretion of the ordinary chondrites. Earth Planet. Sci. Lett. 28, 479–484.

Dodd, R.T., Koffman, D.M., van Schmus, W.R., 1967. A survey of the unequilibrated ordinary chondrites. Geochim. Cosmochim. Acta 31, 935–951.

Dombard, A.J., Barnouin, O.S., Prockter, L.M., Thomas, P.C., 2010. Boulders and ponds on the asteroid 433 Eros. Icarus 210, 713–721.

Drake, M.J., 2001. The Eucrite/Vesta story. Meteorit. Planet. Sci. 36, 501–513.

Durda, D.D., Chapman, C.R., Merline, W.J., Enkse, B.L., 2012. Detecting crater ejecta-blanket boundaries and constraining source crater regions for boulder tracks and elongated secondary craters on Eros. Meteorit. Planet. Sci. 47, 1087–1097. http://dx.doi.org/10.1111/j.1945-5100.2012.01380.x.

Fanale, R.V., Salvail, J.R., 1989. The water regime of asteroid (1) Ceres. Icarus 82, 97–110.
Franzen, M.A., Nichols, S., Bogdon, K., White, C., Godsey, R., Napieralski, N., Benoit, P. H., Sears, D.W.G., 2003. The origin of chondrites: metal silicate separation experiments under microgravity conditions. Geophys. Res. Lett. 30 (14), 4. http://dx.doi.org/10.1029/2003GL017659, SSC 7-1, Cite ID 1780.
Gaffey, M.J., Burbine, T.H., Binzel, R.P., 1993. Asteroid spectroscopy: progress and perspectives. Meteorit. Planet. Sci. 28, 161–187.
Gold, T., Williams, G.J., 1973. Electrostatic transportation of dust on the moon. In: Grard, R.J.L. (Ed.), Photon and Particle Interactions with Surfaces in Space. D. Reidel, Norwell, Massachusetts, p. 557.
Greeley, R., Theilig, E., King, J.S., 1977a. Guide to the geology of Kings Bowl lava field. In: Ronald, Greeley, King, J.S. (Eds.), Volcanism of the Eastern Snake River Plain, Idaho: A Comparative Planetary Guidebook. National Aeronautics and Space Administration, Washington, D.C., pp. 177–188.
Greeley, R., Schultz, P.H., 1977b. Possible planetary analogs to Snake River Plain basalt features. In: Ronald, Greeley, King, J.S. (Eds.), Volcanism of the Eastern Snake River Plain, Idaho: A Comparative Planetary Guidebook. National Aeronautics and Space Administration, Washington, D.C., pp. 233–251.
Grossman, J.N., Alexander, C.M.O.'D., Wang, J., Brearley, A.J., 2000. Bleached chondrules: evidence for widespread aqueous processes on the parent asteroids of ordinary chondrites. Meteorit. Planet. Sci. 35, 467–486.
Haseltine, J.D., Franzen, M.A., Sears, D.W.G., (2006). Fluidization from continuous outgassing as a cause of geological structures on 433 Eros. In: Proceedings of the 37th Annual Lunar and Planetary Science Conference, Abstract no.1103.
Heldmann, J.L., Conley, C.A., Brown, A.J., Fletcher, L., Bishop, J.L., McKay, C.P., 2010. Possible liquid water origin for Atacama Desert mudflow and recent gully deposits on Mars. Icarus 206, 685–690.
Huang, S., Akridge, G., Sears, D.W.G., 1996. Metal-silicate fractionation in the surface dust layers of accreting planetesimals: implications for the formation of ordinary chondrites and the nature of asteroid surfaces. J. Geophys. Res. 101, 29373–29385.
Hughes, S.S., Smith, R.P., Hackett, W.R., Anderson, S.R., 1999. Mafic volcanism and environmental geology of the eastern snake river plain, Idaho. In: Hughes, S.S., Thackray, G.D. (Eds.), Guidebook to the Geology of Eastern Idaho. Idaho Museum of Natural History, Pocatello, Idaho, pp. 143–168.
Hutchison, R., Alexander, C.M.O., Barber, D.J., 1987. The Semarkona meteorite: first recorded occurrence of smectite in an ordinary chondrite, and its implications. Geochim. Cosmochim. Acta 51, 1875–1882.
Jaeger, H.M., Nagel, S.R., 1992. Physics of the granular state. Science 255, 1523–1531.
Jarosewich, E., 1990. Chemical analyses of meteorites—a compilation of stony and iron meteorite analyses. Meteoritics 25, 323–337.
Kareev, M.S., Sears, D.W.G, Benoit, P.H., Thompson, J., Jansma, P., Mattioli, G., 2002. Laboratory simulation experiments and ponds on asteroid 433 Eros (abstract). Lun. Planet. Sci. 33, 1610, Lunar and Planetary Institute, Houston, Texas, USA (CD-ROM).
Kirsimäe, K., Osinski, G.R., 2013w. Impact-induced hydrothermal activity. In: Ozinsky, G.R., Pierazzo, E. (Eds.), In Impact Cratering Processes and Products. Blackwell Publishing, Hoboken, New York, pp. 76–89.
Kienle, J., Kyle, P.R., Self, S., Motyka, R.J., Lorenz, V., 1980. Ukinrek Maars, Alaska, I. April 1977 eruption sequence, petrology and tectonic setting. J. Volcanol. Geotherm. Res. 7, 11–37.
Krohn, K., Jaumann, R., Otto, K., Hoogenboom, T., Wagnera, R., Buczkowski, D.L., Garry, B., Williams, D.A., Yingst, R.A., Scully, J., De Sanctis, M.C., Kneissl, T., Schmedemann, N., Kersten, E., Stephana, K., Matza, K.D., Pieters, C.M., Preusker, F., Roatsch, T., Schenk, P., Russell, C.T., Raymond, C.A., 2015. Mass movement on Vesta at steep scarps and crater rims. Icarus (in press).
Kunii, D., Levensiepel, O., 1991. Fluidization Engineering.
Küppers, M., O'Rourke, L., Bockelée-Morvan, D., Zakharov, V., Lee, S., von Allmen, P., Carry, B., Teyssier, D., Marston, A., Müller, T., Crovisier, J., Antonietta Barucci, M., Moreno, R., 2014. Localized sources of water vapour on the dwarf planet (1) Ceres. Nature 505, 525–527.
Lee, P., 1996. Dust levitation on asteroids. Icarus 124, 181–194.
Marchi, S., Barbieri, C., Küppers, M., Marzari, F., Davidsson, B., Keller, H.U., Besse, S., Lamy, P., Mottola, S., Massironi, M., Cremonese, G., 2010. The cratering history of asteroid (2867) Steins. Planet. Space Sci. 58, 1116–1123.
McCord, T.B., Li, J.Y., Combe, J.P., McSween, H.Y., Jaumann, R., Reddy, V., Tosi, F., Williams, D.A., Blewett, D.T., Turrini, D., Palomba, E., Pieters, C.M., De Sanctis, M.C., Ammannito, E., Capria, M.T., Le Corre, L., Longobardo, A., Nathues, A., Mittlefehldt, D.W., Schröder, S.E., Hiesinger, H., Beck, A.W., Capaccioni, F., Carsenty, U., Keller, H.U., Denevi, B.W., Sunshine, J.M., Raymond, C.A., Russell, C.T., 2012. Dark material on Vesta from the infall of carbonaceous volatile-rich material. Nature 491, 83–86.
McCoy, T.J., Ketchamb, R.A., Wilson, L., Benedix, G.K., Wadhwae, M., Davis, A.M., 2006. Formation of vesicles in asteroidal basaltic meteorites. Earth and Planetary Science Letters 246, 102–108.
McKeever, S.W.S., Sears, D.W., 1980a. Natural thermoluminescence of meteorites—a pointer to orbits? Mod. Geol. 7, 137–145.
Merényi, E., Howel, E.S., Rivkin, A.S., Lebofsky, L.A., 1997. Prediction of water in asteroids from spectral data shortward of 3 μm. Icarus 129, 421–439.
Michel, P., Farinella, P., Froeschle, C., 1998. Dynamics of Eros. Astrophys. J. 116, 2023–2031.
Mills, A.A., 1972. Fluidization on the Moon and planets. In: Runcorn, S.K., Urey, H.C. (Eds.), The Moon, Proceedings from IAU Symposium no. 47. Reidel, Dordrecht, pp. 407–425.
Miyamoto, H., Yano, H., Scheeres, D.J., Abe, S., Barnouin-Jha, O., Cheng, A.F., Demura, H., Gaskell, R.W., Hirata, N., Ishiguro, M., Michikami, T., Nakamura, A.M., Nakamura, R., Saito, J., Sasaki, S., 2007. Regolith migration and sorting on asteroid Itokawa. Science 316, 1011–1014.
Moore, S.R., Franzen, M., Benoit, P.H., Sears, D.W.G., Holley, A., Myers, M., Godsey, R., Czlapinsky, J., 2003. The origin of chondrites: metal-silicate separation experiments under microgravity conditions-II. Geophys. Res. Lett. 30 (10). http://dx.doi.org/10.1029/2002GL016860, Cite ID 1522.
Newsom, H.E., Sewards, T., Keil, K., Graup, G., 1986. Fluidization and hydrothermal alteration of the suevite deposit at the Ries Crater, West Germany, and implications for Mars. J. Geophys. Res. 91, E239–E251.
Osinski, G.R., Grieve, R.A.F., Collins, G.S., Marion, C., Sylvester, P., 2008. The effect of target lithology on the products of impact melting. Meteorit. Planet. Sci. 43, 1939–1954.
Parfitt, E.A., Wilson, L., 2008. Fundamentals of Physical Volcanology. Blackwell Publishing, Malden, MA.
Poppe, A., Horanyi, M., 2010. Simulations of the photoelectron sheath and dust levitation on the lunar surface. J. Geophys. Res. 115, 9. http://dx.doi.org/10.1029/2010JA015286.
Prettyman, T.H., Mittlefehldt, D.W., Yamashita, N., Lawrence, D.J., Beck, A.W., Feldman, W.C., McCoy, T.J., McSween, H.Y., Toplis, M.J., Titus, T.N., Tricarico, P., Reedy, R.C., Hendricks, J.S., Forni, O., Le Corre, L., Li, J.-Y., Mizzon, H., Reddy, V., Raymond, C.A., Russell, C.T., 2012. Elemental mapping by dawn reveals exogenic H in Vesta's regolith. Science 338, 242–246.
Rivkin, A.S., Emery, J.P., 2010. Detection of ice and organics on an asteroidal surface. Nature 464, 1322–1323. http://dx.doi.org/10.1038/nature09028.
Roberts, J.H., Kahn, E.G., Barnouin, O.S., Ernst, C.M., Prockter, L.M., Gaskell, R.W., 2014a. Origin and flatness of ponds on asteroid 433 Eros. Meteorit. Planet. Sci. 49, 1735–1748.
Roberts, J.H., Barnouin, O.S., Kahn, E.G., Prockter, L.M., 2014b. Observational bias and the apparent distribution of ponds on Eros. Icarus 241, 160–164.
Robinson, M.S., Thomas, P.C., Veverka, J., Murchie, S., Carchich, B., 2001. The nature of ponded deposits on Eros. Nature 413, 396–400.
Robinson, M.S., Thomas, P.C., Veverka, J., Murchie, S.L., Wilcox, B.B., 2002. The geology of 433 Eros. Meteorit. Planet. Sci. 37, 1651–1684.
Rubin, A.E., Keil, K., 1984. Size-distributions of chondrule types in the Inman and Allan hills A77011 L3 chondrites. Meteoritics 19, 135–143.
Saito, J., Miyamoto, H., Nakamura, R., Ishiguro, M., Michikami, T., Nakamura, A.M., Demura, H., Sasaki, S., Hirata, N., Honda, C., Yamamoto, A., Yokota, Y., Fuse, T., Yoshida, F., Tholen, D.J., Gaskell, R.W., Hashimoto, T., Kubota, T., Higuchi, Y., Nakamura, T., Smith, P., Hiraoka, K., Honda, T., Kobayashi, S., Furuya, M., Matsumoto, N., Nemoto, E., Yukishita, A., Kitazato, K., Dermawan, B., Sogame, A., Terazono, J., Shinohara, C., Akiyama, H., 2006. Detailed images of asteroid 25143 Itokawa from Hayabusa. Science 312, 1341–1344.
Schneider, D.M., Benoit, P.H., Kracher, A., Sears, D.W.G., 2003. Metal size distributions in EH and EL chondrites. Geophys. Res. Lett. 30 (8), 4. http://dx.doi.org/10.1029/2002GL016672, Cite ID 1420.
Schorghofer, N., 2008. The lifetime of ice on the main belt asteroids. Astrophys. J. 682, 697–705.
Scully, J.E.C., Yin, A., Russell, C.T., Denevi, B.W., Reddy, V., 2012. Potential Transient Liquid Water Flow Features in Fresh Craters on Vesta Fall AGU Meeting. December 3–7.
Scully, J.E.C., Russell, C.T., Yin, A., Jaumann, R., McSween, H.Y., Raymond, C.A., Reddy, V., Le Corre, L., 2013. Gullies on Vesta, related geological features and possible formation mechanisms. In: Proceedings of the 44th Lunar and Planetary Science Conference, #1796 (Abstract).
Sears, D.W.G., 2005. Chondrules and Chondrites. Cambridge University Press, Cambridge, UK.
Sears, D.W.G., Chittenden, J.D., 2005. On laboratory simulation and the temperature dependence of the evaporation rate of brine on Mars. Geophys. Res. Lett. 32 (23), 4.
Sears, D.W.G., Moore, S.R., 2005. On laboratory simulation and the evaporation rate of water on Mars. Geophys. Res. Lett. 32 (16), 4.
Sears, D.W., Grossman, J.N., Melcher, C.L., Ross, L.M., Mills, A.A., 1980a. Measuring the metamorphic history of unequilibrated ordinary chondrites. Nature 287, 791–795.
Sears, D.W.G., Kochan, H., Huebner, W.F., 1999. Simulation experiments and surface processes on comets. Meteorit. Planet. Sci. 34, 497–525.
Stöffler, D., Artemieva, N.A., Wünnemann, K., Reimold, W.U., Jacob, J., Hansen, B.K., Summerson, I.A.T., 2013. Ries crater and suevite revisited—observations and modeling Part I: observations. Meteorit. Planet. Sci. 48, 515–589.
Stubbs, T.J., Vondrak, R.R., Farrell, W.M., 2005. A dynamic fountain model for lunar dust. Adv. Space Res. 37, 59–66.
Thomas, P.C., Veverka, J., Robinson, M.S., Murchie, S., 2001. Shoemaker crater as the source of most ejecta blocks on the asteroid 433 Eros. Nature 413, 394–396.
Thomas, P., A'Hearn, M., Belton, M.J.S., Brownlee, D., Carcich, B., Hermalyn, B., Klaasen, K., Sackett, S., Schultz, P.H., Veverka, J., Bhaskaran, S., Bodewits, D., Chesley, S., Clark, B., Farnham, T., Groussin, O., Harris, A., Kissel, J., Li, J.-Y., Meech, K., Melosh, J., Quick, A., Richardson, J., Sunshine, J., Wellnitz, D., 2013. The nucleus of comet 9P/Tempel 1: shape and geology from two flybys. Icarus 222, 453–466.
Thomas, N., Sierks, H., Barbieri, C., Lamy, P.L., Rodrigo, R., Rickman, H., Koschny, D., Keller, H.U., Agarwal, J., A'Hearn, M.F., Angrilli, F., Auger, A.T., Barucci, M.A., Bertaux, J.-L., Bertini, I., Besse, S., Bodewits, D., Cremonese, G., Da Deppo, V., Davidsson, B., De Cecco, M., Debei, S., El-Maarry, M.R., Ferri, F., Fornasier, S., Fulle, M., Giacomini, L., Groussin, O., Gutierrez, P.J., Güttler, C., Hviid, S.F., Ip, W.-H., Jorda, L., Knollenberg, J.,

Kramm, J.S., Kührt, E., Küppers, M., Forgia, F.La, Lara, L.M., Lazzarin, M., LopezM, J.J., Magrin, S., Marchi, S., Marzari, F., Massironi, M., Michalik, H., Moissl, R., Mottola, S., Naletto, G., Oklay, N., Pajola, M., Pommerol, A., Preusker, F., Sabau, L., Scholten, F., Snodgrass, C., Tubiana, C., Vincent, J.-B., Wenzel, K.-P., 2015. The morphological diversity of comet 67P/Churyumov–Gerasimenko. Science 347, aaa04440-1–aaa04440-6.

Tornabene, L.L., Osinski, G.R., McEwen, A.S., Boyce, J.M., Bray, V.J., Caudill, C.M., Grant, J.A., Hamilton, C.W., Mattson, S., Mouginis-Mark, P.J., 2012. Widespread crater-related pitted materials on Mars: further evidence for the role of target volatiles during the impact process. Icarus 220, 348–368.

Van Schmus, W.R., Wood, J.A., 1967. A chemical-petrologic classification for the chondritic meteorites. Geochim. Cosmochim. Acta 31, 747–765.

Viateau, B., Rapaport, M.R., 2001. Mass and density of asteroids (4) Vesta and (11) Parthenope. Astron. Astrophys. 370, 602–609. http://dx.doi.org/10.1051/0004-6361:20010222.

Villas, F., 1994. A cheaper, faster, better was to detect water of hydration on solar system bodies. Icarus 111, 456–467.

Vincent, J.B., Besse, S., Marchi, S., Sierks, H., Massironi, M., 2012. Physical properties of craters on asteroid (21) Lutetia. Planet. Space Sci. 66, 79–86.

Whipple, F.L., 1972a. Accumulation of chondrules on asteroids. Physical Studies of Minor Planets, 267. NASA Special Publication, Washington, D.C., pp. 251–262.

Whipple, F.L., 1972b. On certain aerodynamic processes for asteroids and comets. In: Elvius, A. (Ed.), From Plasma to Planet, Nobel Symposium 21. Wiley, Hoboken, New Jersey, pp. 211–232.

Wiik, H.B., 1969. On regular discontinuities in the composition of meteorites. Comment. Phys. Math. 34, 135–145.

Wilkening, L., 1973. Foreign inclusions in stony meteorites I. Carbonaceous chondritic zenoliths in the Kapoeta howardite. Geochim. Cosmochim. Acta 37, 1955–1989.

Wilson, C.J.N., 1980. The role of fluidization in the emplacement of pyroclastic flows: an experimental approach. J. Volcanol. Geotherm. Res. 8, 231–249.

Womer, M.B., 1977. The origin of Split Butte, a maar type crater of the south-central Snake River Plain. In: Ronald, Greeley, King, J.S. (Eds.), Volcanism of the Eastern Snake River Plain, Idaho: A Comparative Planetary Guidebook. National Aeronautics and Space Administration, Washington, D.C., pp. 189–202.